PHYSICAL REVIEW C **86**, 021602(R) (2012)

Elastic proton scattering of medium mass nuclei from coupled-cluster theory

G. Hagen[1,2] and N. Michel[2]
[1]*Physics Division, Oak Ridge National Laboratory, Oak Ridge, Tennessee 37831, USA*
[2]*Department of Physics and Astronomy, University of Tennessee, Knoxville, Tennessee 37996, USA*
(Received 11 June 2012; revised manuscript received 24 July 2012; published 13 August 2012)

Using coupled-cluster theory and interactions from chiral effective field theory, we compute overlap functions for transfer and scattering of low-energy protons on the target nucleus ^{40}Ca. Effects of three-nucleon forces are included phenomenologically as in-medium two-nucleon interactions. Using known asymptotic forms for one-nucleon overlap functions we derive a simple and intuitive way of computing scattering observables such as elastic scattering phase shifts and cross sections. As a first application and proof of principle, we compute phase shifts and differential interaction cross sections at energies of 9.6 and 12.44 MeV and compare with experimental data. Our computed diffraction minima are in fair agreement with experimental results, while we tend to overestimate the cross sections at large scattering angles.

DOI: 10.1103/PhysRevC.86.021602 PACS number(s): 21.10.Tg, 24.10.Cn, 24.50.+g

Introduction. With the advent of accelerators of new generation, which provide radioactive ion beams, it becomes possible to synthesize nuclei far from the valley of stability. Little is known about these nuclei. For example, the nuclear interaction is not well understood at large proton-to-neutron ratios, and it appears that its effects are radically different close to driplines compared to the vicinity of the valley of stability. The most striking example is the redistribution of shell closures, which are different from the usual magic numbers present in well-bound nuclei [1,2]. In order to precisely study nuclei close to driplines, new theoretical tools must be developed, going further from the standard structure methods of nuclear analysis, based on the use of standard shell model, treating all nuclear states as well bound, and, in reaction theory, using optical potentials fitted from experimental data. Indeed, both nuclear structure and reactions must be unified, so that both internucleon correlations and scattering degrees of freedom are included within the same framework [3]. Microscopic models aiming at unifying nuclear structure and reactions date back to the seminal works of Chew [4], Watson [5], and Kerman, McManus, and Thaler, who sought to find a microscopic basis for phenomenological optical potentials [6]. More recently, the full-folding g-matrix approach by Amos and collaborators [7] and the full-folding optical potential model by Elster, Weppner, and Chinn [8] have had great success in determining the optical potential from microscopic input. Nevertheless, all these approaches rely on approximations such as the impulse approximation and simplified density matrices of the target nucleus. Because of the increase of computational power in the past few years, *ab initio* reaction frameworks have started to emerge and hold great promise. The resonating group method within the no core shell model has successfully described nucleon and deuteron scattering and fusion in light nuclei [9], the Green's function Monte Carlo method has been used to describe elastic scattering on ^{4}He and in the computation of asymptotic normalization coefficients in light nuclei [10], and finally the self-consistent Green's function (SCGF) method has been applied to the microscopic calculation of optical potentials and proton scattering on ^{16}O [11].

An interesting avenue for computing nuclear reactions microscopically lies in coupled-cluster theory. The coupled-cluster method is a microscopic theory which comes at a relatively low computational cost and at the same time can provide accurate descriptions of low-lying states and properties of nuclei with closed (sub-)shells [12,13]. Recently, the coupled-cluster method has made significant progress in computing structures of nuclei from the valley of stability towards the neutron dripline. Using a Berggren basis [14] consisting of bound, resonant, and scattering states, both loosely bound and unbound states have been accurately computed within the coupled-cluster formalism [15,16]. However, so far no attempt has been made to apply the coupled-cluster method to compute reaction observables, and it is the aim of this work to fill this gap and to develop a new formalism to compute reaction observables such as elastic scattering cross sections using microscopic coupled-cluster theory. As a first application we consider the elastic scattering reaction ^{40}Ca(p,p)^{40}Ca, whose phase shifts and differential elastic cross sections are evaluated at low energies.

Hamiltonian and treatment of the infinite-range Coulomb interaction. The intrinsic $A-$nucleon Hamiltonian consists of kinetic, nuclear, and Coulomb parts,

$$\hat{H} = \sum_{1\leqslant i<j\leqslant A} \left(\frac{(\vec{p}_i - \vec{p}_j)^2}{2mA} + \hat{V}_{NN}^{(i,j)} + \hat{V}_{\text{Coul}}^{(i,j)} + \hat{V}_{\text{3Neff}}^{(i,j)} \right). \quad (1)$$

Here, the intrinsic kinetic energy depends on the mass number A. The potential $\hat{V}_{NN}$ denotes the chiral NN interaction at next-to-next-to-next-to-leading order [17,18] (with cutoff $\Lambda = 500$ MeV), $\hat{V}_{\text{Coul}}$ is the Coulomb interaction, and $\hat{V}_{\text{3Neff}}$ is a schematic potential based on the in-medium chiral NN interaction by Holt *et al.* [19]. The potential $\hat{V}_{\text{3Neff}}$ results from integrating one nucleon in the leading-order chiral 3NF over the Fermi sphere with Fermi momentum k_F in symmetric nuclear matter. It depends formally on the Fermi momentum k_F, the low-energy constants c_D and c_E of the short-range contributions to the leading-order chiral 3NF, and the chiral cutoff. The latter is equal to the value employed in the chiral NN interaction [18]. In this work we employ the parameters

$k_F = 0.95$ fm^{-1}, $c_D = -0.2$, and $c_E = 0.735$, which was recently applied for the study of shell evolution in neutron-rich calcium isotopes [1].

Let us briefly discuss our treatment of the short- and long-range parts of the Hamiltonian in Eq. (1). The nuclear interaction $\hat{V}_{NN}$ is of short range and is adequately expanded in a basis of harmonic oscillator states (see Ref. [20] for details). The difficulty induced by the infinite-range character of the Hamiltonian is thus embodied in the Coulomb interaction $\hat{V}_{\rm Coul}$, asymptotically behaving as $(Z-1)e^2/r$, with r the distance between the isolated proton and the center of charge of the remaining part of the nucleus. Clearly, it is insufficient to treat $\hat{V}_{\rm Coul}$ with a harmonic oscillator expansion as we do for $\hat{V}_{NN}$. A solution to this problem has been formulated in Ref. [21]. For this, the Coulomb interaction is rewritten as the sum of two terms:

$$V_{\rm Coul} = U_{\rm Coul}(r) + [V_{\rm Coul} - U_{\rm Coul}(r)], \tag{2}$$

where one demands that the Coulomb one-body potential $U_{\rm Coul}(r)$ behave as $(Z-1)e^2/r$ for $r \to +\infty$. In this work we choose $U_{\rm Coul}(r) = {\rm erf}(\alpha r)(Z-1)e^2/r$, where erf is the error function and $\alpha = \pi/4{\rm fm}^{-1}$. Thus, the $[V_{\rm Coul} - U_{\rm Coul}(r)]$ term is short ranged, so that one can use the harmonic oscillator expansion method of Ref. [20] to calculate its matrix elements. Note that the r coordinate can be taken with respect to the origin of the laboratory, because center-of-charge effects are negligible in the asymptotic region on the one hand and for a medium-mass nucleus such as ^{40}Ca on the other hand.

In order to account for the scattering continuum using the coupled-cluster formalism, it is convenient to express the Hamiltonian for given partial waves in a basis of spherical Bessel functions [16]. Thus, in order to proceed, we express $U_{\rm Coul}(r)$ in momentum space, and write it in the following way:

$$U_{\rm Coul}(k,k') = \langle k|U_{\rm Coul}(r) - \frac{(Z-1)e^2}{r}|k'\rangle + \frac{(Z-1)e^2}{\pi} Q_\ell\left(\frac{k^2+k'^2}{2kk'}\right), \tag{3}$$

where ℓ is the orbital angular momentum of the considered partial wave and Q_ℓ is the Legendre function of the second kind [22]. As the the first term of Eq. (3) decreases very quickly for $r \to +\infty$, it can be calculated by numerical integration. However, the second term presents a logarithmic singularity at $k = k'$. In order to counter this state of affairs, we follow the off-diagonal method introduced in Ref. [23]. It consists of replacing the infinite value $Q_\ell(1)$ in Eq. (3) occurring at $k = k'$ with a finite value depending on the discretization used (see Ref. [23] for method and details).

In order to show the precision of the method in the context of momentum space calculation, we diagonalize with a basis of Bessel functions the one-body Hamiltonian for the $\ell = 0$ partial wave studied in Ref. [23], which reads

$$h = \frac{\hat{p}^2}{2m} - V_o\left[1 + \exp\left(\frac{r-R_0}{d}\right)\right]^{-1} + U_{\rm Coul}(r), \tag{4}$$

where m is the proton mass, $d = 0.65$ fm, $R_0 = 3$ fm, $V_o = 52$ MeV, and $U_{\rm Coul}(r)$ is the Coulomb potential from Ref. [20].

Obtained scattering wave functions have been fitted for large r with their asymptotic limit equal to

$$C_F \frac{F(\ell,\eta,kr)}{r} + C_G \frac{G(\ell,\eta,kr)}{r}, \tag{5}$$

where $F(\ell,\eta,x)$ and $G(\ell,\eta,x)$ are respectively the regular and irregular Coulomb wave functions [22], η is the Sommerfeld parameter, and C_F and C_G are integration constants. Regular and irregular Coulomb wave functions are evaluated numerically using the publicly available CWFCOMPLEX code [24], while C_F and C_G constants are determined by fitting Eq. (5) to the considered scattering wave functions at $r = 10$ fm. Results are depicted in Fig. 1. It is therein clear that their asymptotic behavior is very well reproduced, as Coulomb asymptotic expansions and diagonalized scattering wave functions are virtually indistinguishable for $r > 7$ fm. This proves that the infinite-range character of the Coulomb interaction can be handled precisely with Fourier-Bessel transform, so that reactions involving protons, such as elastic scattering, can be undertaken.

One-nucleon overlap functions and coupled-cluster theory. The scattering of a nucleon on a target A can be described by the one-nucleon overlap function. The one-nucleon radial overlap function $O_A^{A+1}(lj;r)$ is defined microscopically as the overlap between two independent many-nucleon wave functions of A and $A+1$ nucleons,

$$O_A^{A+1}(lj;kr) = \sum\!\!\!\!\!\!\int_n \langle A+1||\tilde{a}^\dagger_{nlj}||A\rangle \phi_{nlj}(r). \tag{6}$$

The double bar denotes a reduced matrix element, and the integral-sum over n represents both the sum over the discrete spectrum and an integral over the corresponding continuum part of the spectrum. The creation operator $\tilde{a}^\dagger_{nlj}$ is a spherical tensor of rank j. The radial single-particle basis function is given by the term $\phi_{nlj}(r)$, where l and j denote the single-particle orbital and angular momentum, respectively, and n is the nodal quantum number. The isospin quantum number has

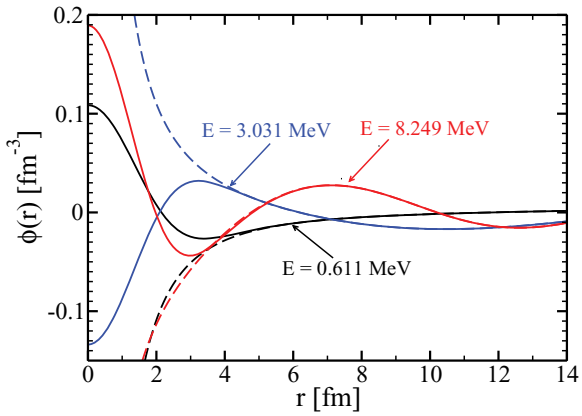

FIG. 1. (Color online) Scattering s-wave functions $\varphi(r)$ obtained from diagonalization of the one-body Hamiltonian defined in Eq. (4) in momentum space (solid lines) and their asymptotic expansion defined in Eq. (5) (dashed lines) as a function of radius, provided in femtometers. Wave functions are given in units of femtometers^{-3} and their energy is written on the figure in units of million electron volts.

been suppressed. The one-nucleon overlap function describes the capture or scattering of an incoming particle with quantum numbers lj on the target nucleus A and with the final state $A+1$ being either a bound or a scattering state. The momentum k is given from the energy difference $k=\sqrt{2\tilde{m}(E^{A+1}-E^{A})}/\hbar$, in the case of A and $A+1$ being in their ground state. $E^{A+1}-E^{A}$ is the one-nucleon separation energy in the $A+1$ nucleus (here $\tilde{m}=(1-1/A)m$). We emphasize that the overlap function is defined microscopically and independently of the single-particle basis. It is uniquely determined by the many-body wave functions $|A\rangle$ and $|A+1\rangle$. $|A\rangle$ and $|A+1\rangle$ can in general either be in their ground or any excited state. However, in this work we are interested in low-energy elastic scattering, which implies that the target nucleus $|A\rangle$ is in its ground state before and after the scattering. The one-nucleon overlap functions are formally solutions of the Dyson equation, which can be written in a Schrödinger-like form where the self-energy takes the place of a nonlocal and energy-dependent optical potential [11]. Outside the range R of the optical potential, the one-nucleon overlap functions for bound $A+1$ states takes ($k=i\kappa$) the form

$$O_A^{A+1}(lj;kr)=C_{lj}(i\kappa)\frac{W_{-\eta,l+1/2}(i\kappa r)}{r} \tag{7}$$

and for $A+1$ scattering states ($k>0$),

$$O_A^{A+1}(lj;kr)=B_{lj}(k)\left[F_{l,\eta}(kr)-\tan\delta_l(k)G_{l,\eta}(kr)\right]. \tag{8}$$

Here $W_{-\eta,l+1/2}$ is the Whittaker function, $F_{l,\eta}$ and $G_{l,\eta}$ are the regular and irregular Coulomb wave functions, η is the Sommerfeld parameter [$\eta=(Z-1)e^2\sqrt{\tilde{m}/2|E|}$], $C_{lj}(i\kappa)$ is the asymptotic normalization coefficient (ANC), $\tan\delta_l(k)$ is the lth partial wave scattering phase shift at momentum k, and $B_{lj}(k)$ is an arbitrary normalization constant for the scattering states. In order to compute the phase shifts at a given energy, it is sufficient to know the one-nucleon overlap function $O_A^{A+1}(lj;kr)$ and its derivative at a given radius $r>R$. In order to obtain $O_A^{A+1}(lj;kr)$ we need to solve for the ground state of the target nucleus A and the ground and excited scattering states in the residual nucleus $A+1$. The coupled-cluster method is a very efficient tool for the computation of ground and low-lying excited states in nuclei with a closed (sub-)shell structure and their neighbors. In this work the target nucleus A is a closed-shell nucleus, and we use the coupled-cluster method to compute the ground state of A, that is, $|A\rangle=e^{T}|\phi_A\rangle$. Here $|\phi_A\rangle$ is the Hartree-Fock reference state while T is a linear combination of particle-hole excitation operators. For the residual $A+1$ nucleus we use particle-attached equation-of-motion coupled-cluster theory to obtain the ground and excited states, and the $A+1$ wave functions are therefore given by $\langle A+1|_\mu=\langle\phi_A|L_\mu^{A+1}e^{-T}$, with L_μ^{A+1} a linear combination of one-particle and two-particle–one-hole de-excitation operators (details on our implementation are presented in Refs. [25,26]). Inserting these expressions for the A and $A+1$ systems into Eq. (6), we obtain the coupled-cluster formulation of the one-nucleon overlap functions:

$$O_A^{A+1}(lj;kr)=\sum_n\!\!\!\!\!\!\int\langle\phi_A|\left|L_\mu^{A+1}\overline{\tilde{a}_{nlj}^{\dagger}}\right||\phi_A\rangle\phi_{nlj}(r). \tag{9}$$

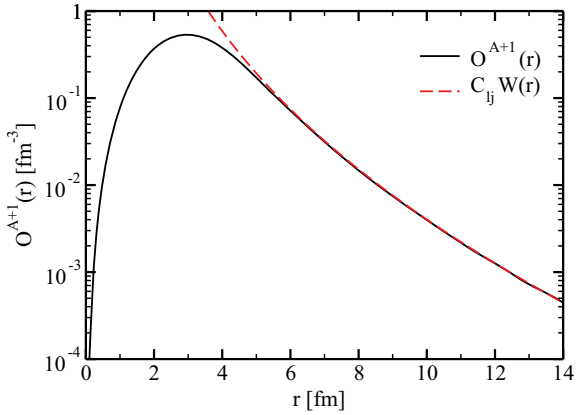

FIG. 2. (Color online) Radial overlap function $O_A^{A+1}(lj;kr)$ between the ground state of ^{40}Ca and the $J^\pi=7/2^-$ ground state of ^{41}Sc (solid line), also shown is the corresponding Whittaker function $C_{lj}W_{-\eta,l+1/2}(i\kappa r)/r$ for the $f_{7/2}$ proton partial wave (dashed line).

Here $\overline{\tilde{a}_{nlj}^{\dagger}}=e^{-T}\tilde{a}_{nlj}^{\dagger}e^{T}$ is the similarity-transformed creation operator. The derivation of the diagrammatic and algebraic expressions of Eq. (9) and $\overline{\tilde{a}_{nlj}^{\dagger}}$ can be found in Ref. [27]. Note that in order to compute the radial overlap in Eq. (9) we need to use the same mass number (41) in the intrinsic kinetic energy of the A and $A+1$ Hamiltonians in Eq. (1). This introduces a small error in the ground state of the target nucleus A. However, this error decreases rapidly with increasing mass, and we estimate that the error is of the order of 100–200 keV in the relative energy entering the overlap function [28].

In our coupled-cluster calculations we use a model space consisting of $N_{\max}=17$ major spherical oscillator shells with the oscillator frequency $\hbar\omega=26$ MeV. This is a sufficiently large model space to reach practically converged results for the ground state of ^{40}Ca (see Ref. [1]). In order to properly account for scattering continuum in ^{41}Sc we use a Gamow-Hartree-Fock basis [29] for the relevant proton partial waves. In constructing the single-particle basis with the correct treatment of long-range Coulomb effects, we use the off-diagonal method in momentum space and discretize the one-body momentum space Schrödinger equation with 50 mesh points. We find that this is a sufficiently large number of mesh points in order to obtain the correct Coulomb asymptotics necessary to describe proton elastic scattering on ^{40}Ca.

Results. Figure 2 shows the computed radial overlap function for the ground state of ^{40}Ca with the $J^\pi=7/2^-$ ground state of ^{41}Sc on a logarithmic scale. Our computed proton separation energy for ^{41}Sc is $S_{\rm p}^{\rm CC}=0.71$ MeV, which is in good agreement with the experimental proton separation energy $S_{\rm p}^{\rm Exp}=1.09$ MeV. From the radial overlap function and the separation energy we can compute the behaviour of the the overlap function at distances beyond the range of the nuclear interaction according to Eq. (7). It is clearly seen that the overlap function and the known asymptotic form completely overlap for distances larger than $r\sim 8$ fm. Figure 3 shows the computed radial overlap functions for the ground state of ^{40}Ca with two $J^\pi=7/2^-$ scattering states of ^{41}Sc, at the energies $E=5.439$ MeV and $E=16.304$ MeV,

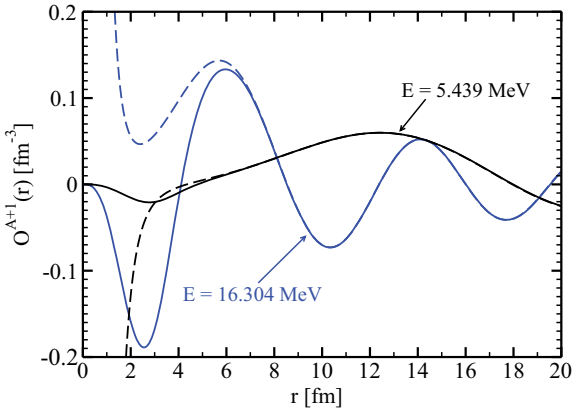

FIG. 3. (Color online) Radial overlap functions $O_A^{A+1}(lj;kr)$ between the ground state of ^{40}Ca and two $J^\pi = 7/2^-$ scattering states in ^{41}Sc (solid lines). Also shown are the corresponding Coulomb scattering functions $B_{lj}(k)[F_{l,\eta}(kr) - \tan\delta_l(k)G_{l,\eta}(kr)]$ (dashed lines).

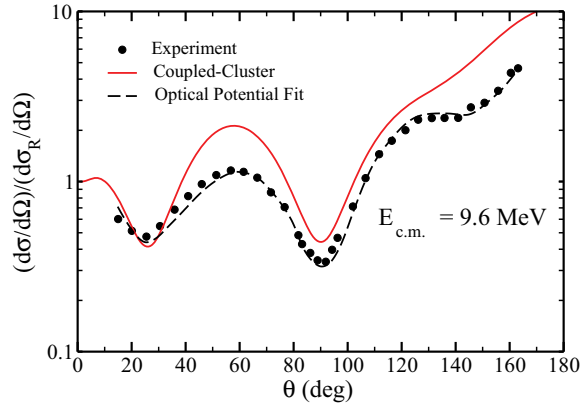

FIG. 5. (Color online) Differential cross section from coupled-cluster calculations divided by Rutherford cross section for elastic proton scattering on ^{40}Ca at $E_{\rm cm} = 9.6$ MeV (solid line), experimental data (dots), and optical model potential fits (dashed line), taken from Ref. [31].

respectively. As we found for the bound overlap function shown in Fig. 2, we see that the radial overlap function for scattering states and the known asymptotic forms completely overlap for distances larger than $r \sim 8$ fm. By matching the asymptotic forms of the overlap functions given in Eq. (8) with the computed overlap functions, it is clear that we can determine the corresponding elastic scattering phase shift at the computed scattering energy. Figure 4 shows our computed scattering phase shifts for proton elastic scattering on ^{40}Ca for the $s_{1/2}$, $p_{1/2}$, $p_{3/2}$, $d_{3/2}$, $d_{5/2}$ partial waves at energies below 14 MeV. The solid dots correspond to the computed scattering energies, and we used cubic spline to interpolate between the discrete set of scattering energies. We clearly see the appearance of a narrow resonance in the $p_{3/2}$ partial wave around ∼1.6 MeV, while a broader resonance appears in the $p_{1/2}$ partial wave at around ∼3.4 MeV. In order to check our results we computed the low-lying resonances in ^{41}Sc using a complex Gamow-Hartree-Fock basis [16], and we found a $J^\pi = 3/2^-$ resonance at the energy $E = 1.61–0.001i$ MeV and a $J^\pi = 1/2^-$ resonance at the energy $E = 3.42–0.20i$ MeV. Clearly these energies are consistent with the resonances appearing in the $p_{3/2}$ and $p_{1/2}$ elastic scattering phase shifts in Fig. 4. From the scattering phase shifts we can compute the differential cross section for elastic proton scattering as described in, for example, Ref. [30]. Figures 5 and 6 show our computed differential cross section divided by the Rutherford cross section for elastic proton scattering on ^{40}Ca at the relative center-of mass energies $E_{\rm cm} = 9.6$ MeV and $E_{\rm cm} = 12.44$ MeV, and we compare to these experimental results and the optical model potential fit to data of Ref. [31]. All partial waves for $l \leqslant 2$ were included in the computation of the cross sections. In light of the fact that we performed no fine-tuning of model parameters to scattering data in ^{40}Ca, we get overall fair agreement between our calculated cross sections and the experimental cross sections. In particular we see that our computed minima are in good agreement with the experimental minima, while we tend to overestimate the cross sections at large scattering angles. The overestimated cross sections at large angles is most likely due to the fact that we do not account for intermediate excitations that takes place above the deuteron

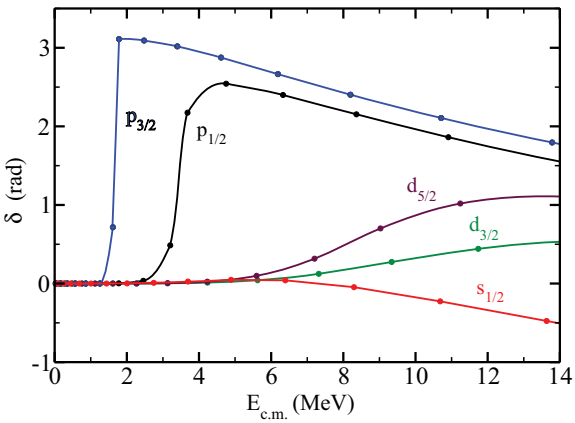

FIG. 4. (Color online) Computed phase shifts for elastic proton scattering on ^{40}Ca for low-lying partial waves and energies below 14 MeV.

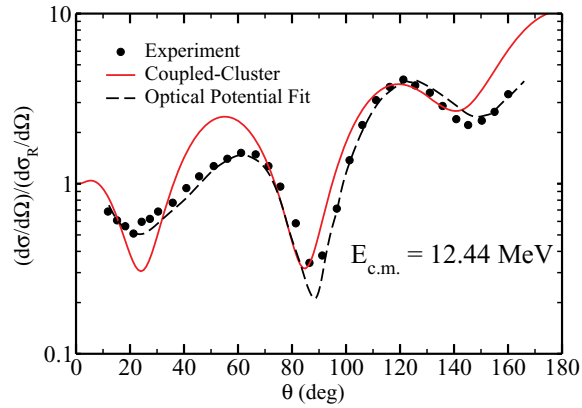

FIG. 6. (Color online) Same caption as in Fig. 5 except that the energy is $E_{\rm cm} = 12.44$ MeV.

threshold, and these excitations generally cause absorption and reduce the cross section at large angles. Going beyond $2p$-$1h$ excitations for the computation of the $A+1$ wave functions will account for such effects, and we are working towards such improvements in our approach. We also computed the cross sections including the $f_{5/2}$, $f_{7/2}$, $g_{7/2}$, $g_{9/2}$ partial waves; however, the agreement with data did not improve. This is most likely due to the fact that our computations for the $f_{5/2}$ and $g_{9/2}$ partial waves find very narrow resonances at energies that are too low as compared to the experiment. This is also consistent with the ∼10-MeV overbinding we get for ^{40}Ca using the Hamiltonian in Eq. (1) [1]. As cross sections at low energies are very sensitive to the location of low-lying resonances, we believe that the disagreement between data and theory is most likely due to (i) deficiencies in the Hamiltonian and (ii) the approximation of the $A+1$ wave function.

Conclusions. Using coupled-cluster theory, we computed cross sections for elastic scattering of protons on ^{40}Ca, at the center-of-mass energies 9.6 and 12.44 MeV, respectively. We found a fair agreement for our computed diffraction minima with experiment, while we tend to overestimate the cross sections at large scattering angles. The key ingredients for computing observables for proton scattering are (i) the one-nucleon overlap function computed from microscopic coupled-cluster theory and (ii) a single-particle basis that has the correct Coulomb asymptotics. We showed that the newly developed *off-diagonal* method is a very accurate method for computing Coulomb scattering wave functions in momentum space. The fast convergence of the scattering wave functions with increasing number of mesh points makes this basis an ideal starting point for computing reaction observables. This work constitutes a successful application of coupled-cluster theory to nuclear reactions, and we believe it makes a significant leap forward in linking reactions with microscopic structure calculations.

Acknowledgments. We acknowledge valuable discussions with T. Papenbrock and F. Nunes. This work was supported by the Office of Nuclear Physics, U.S. Department of Energy (Oak Ridge National Laboratory). This work was supported in part by the U.S. Department of Energy under Grants No. DE-FG02-03ER41270 (University of Idaho), No. DE-FG02-96ER40963 (University of Tennessee), and No. DE-FC02-07ER41457 (UNEDF SciDAC). This research used computational resources of the National Center for Computational Sciences at the National Institute for Computational Sciences.

[1] G. Hagen, M. Hjorth-Jensen, G. R. Jansen, R. Machleidt, and T. Papenbrock, Phys. Rev. Lett. **109**, 032502 (2012).
[2] B. Fernández-Domínguez *et al.*, Phys. Rev. C **84**, 011301 (2011); D. Suzuki *et al.*, Phys. Rev. Lett. **103**, 152503 (2009); E. Becheva *et al.*, *ibid.* **96**, 012501 (2006).
[3] J. Dobaczewski *et al.*, Prog. Part. Nucl. Phys. **59**, 432 (2007).
[4] F. Chew, Phys. Rev. **80**, 196 (1951).
[5] K. M. Watson, Phys. Rev. **89**, 575 (1953).
[6] A. K. Kerman, H. McManus, and R. M. Thaler, Ann. Phys. **8**, 551 (1959).
[7] K. Amos *et al.*, Adv. Nucl. Phys. **25**, 275 (2000).
[8] Ch. Elster, S. P. Weppner, and C. R. Chinn, Phys. Rev. C **56**, 2080 (1997).
[9] P. Navrátil and S. Quaglioni, Phys. Rev. Lett. **108**, 042503 (2012); S. Quaglioni and P. Navrátil, *ibid.* **101**, 092501 (2008).
[10] K. M. Nollett and R. B. Wiringa, Phys. Rev. C **83**, 041001 (2011); K. M. Nollett, S. C. Pieper, R. B. Wiringa, J. Carlson, and G. M. Hale, Phys. Rev. Lett. **99**, 022502 (2007).
[11] H. Dussan, S. J. Waldecker, W. H. Dickhoff, H. Muther, and A. Polls, Phys. Rev. C **84**, 044319 (2011); C. Barbieri and B. K. Jennings, *ibid.* **72**, 014613 (2005).
[12] F. Coester, Nucl. Phys. **7**, 421 (1958); F. Coester and H. Kümmel, *ibid.* **17**, 477 (1960); J. Čížek, J. Chem. Phys. **45**, 4256 (1966); Adv. Chem. Phys. **14**, 35 (1969); H. Kümmel, K. H. Lührmann, and J. G. Zabolitzky, Phys. Rep. **36**, 1 (1978).
[13] R. J. Bartlett and M. Musiał, Rev. Mod. Phys. **79**, 291 (2007).
[14] T. Berggren, Nucl. Phys. A **109**, 265 (1968).
[15] G. Hagen *et al.*, Phys. Lett. B **656**, 169 (2007).
[16] G. Hagen, T. Papenbrock, and M. Hjorth-Jensen, Phys. Rev. Lett. **104**, 182501 (2010).
[17] R. Machleidt and D. R. Entem, Phys. Rep. **503**, 1 (2011).
[18] D. R. Entem and R. Machleidt, Phys. Rev. C **68**, 041001(R) (2003).
[19] J. W. Holt, N. Kaiser, and W. Weise, Phys. Rev. C **79**, 054331 (2009); **81**, 024002 (2010).
[20] G. Hagen, M. Hjorth-Jensen, and N. Michel, Phys. Rev. C **73**, 064307 (2006).
[21] N. Michel, W. Nazarewicz and M. Płoszajczak, Phys. Rev. C **82**, 044315 (2010).
[22] M. Abramowitz and I. A. Stegun (eds.) *Handbook of Mathematical Functions with Formulas, Graphs, and Mathematical Tables* (Dover Publications, New York, 1972).
[23] N. Michel, Phys. Rev. C **83**, 034325 (2011).
[24] N. Michel, Comput. Phys. Comm. **176**, 23 (2007).
[25] G. Hagen, T. Papenbrock, D. J. Dean, and M. Hjorth-Jensen, Phys. Rev. Lett. **101**, 092502 (2008).
[26] G. Hagen, T. Papenbrock, D. J. Dean, and M. Hjorth-Jensen, Phys. Rev. C **82**, 034330 (2010).
[27] Ø. Jensen *et al.*, Phys. Rev. C **82**, 014310 (2010).
[28] G. Hagen, M. Hjorth-Jensen, G. R. Jansen, R. Machleidt, and T. Papenbrock, Phys. Rev. Lett. **108**, 242501 (2012).
[29] N. Michel *et al.*, J. Phys. G **36**, 013101 (2009).
[30] I. J. Thompson, Comput. Phys. Rep. **7**, 167 (1988).
[31] W. T. H. van Oers, Phys. Rev. C **3**, 1550 (1971).